

Supplementary Notes

1 Advantages to oscillatory stimulation approach

Because of the way we defined T_{\max} , our results automatically extend to an infinite set of variations of each explicit circuit model we studied (Fig. 1 K). These variations do not change T_{\max} . Therefore, by analyzing representative models (Fig. S2), we studied all related variants (Fig. 1 K): i) Each model is trivially equivalent to other models by rescaling the variables, which is why we studied $S = 0$ or $= 1$ only. ii) Nodes that merely delay signals anywhere along the signal transduction pathway do not change T_{\max} as long as the final inputs U_m and U_n in Fig. 1 K are simultaneous. iii) Upstream nodes (from S to U_m and U_n in Fig. 1 K) that nonlinearly transform the input do not change the on-off stimulus except for rescaling. Therefore, our scheme is, in principle, robust to nonlinearities upstream of the adaptation mechanism. iv) Furthermore, repeated input pulses permit us to take advantage of a simple trick: The time average of the output $O(d, T)$ is directly proportional to the time average of further upstream elements in the signal transduction cascade, if the intervening nodes have first-order kinetics ($\dot{W}_i = k_{i,+}W_{i-1} - k_{i,-}W_i$ implies that $\langle W_i \rangle$ is proportional to $\langle W_{i-1} \rangle$). This means that we only needed to analyze explicitly circuits whose output passed through nonlinear filters (up to V_p in Fig. 1 K) and we could neglect further downstream nodes with first-order dynamics. Also, this means that in practice, the measured output does not need to be deconvolved mathematically to reconstruct the underlying responses as long as the intervening processes are first-order, for example, folding and maturation of reporter fluorescent proteins can be ignored⁴⁴. v) Lastly, in each numerical calculation, we explicitly modeled the dynamics of $O(t)$ with Michaelis-Menten and Hill coefficients as a function of $R(t)$, for example, to represent GCaMP Ca^{2+} binding cooperativity⁴⁰. The explicitly modeled nonlinearities could represent multiple successive output nonlinearities, e.g., $V_1 = R^2$ and $\dot{O} = V_1/(1 + V_1/V_0) - \lambda_O O$ (Fig. 1 K).

Other advantages to using periodic stimuli and measuring the average of the output are that transients and the dependence on initial conditions disappear in many dynamical systems with repeated pulsing⁴⁵; the mathematical description and the analysis of the system simplify, for example, initial conditions become irrelevant. Also, the time average of the output is less susceptible to random measurement noise than any particular point in a recording, e.g., the height of a peak.

2 Mathematical proofs for no period skipping in IFFLs

2.1 Feedforward systems

We begin by considering purely feedforward systems (such as the IFFL in Fig. 1 E, I), where the dynamical elements $\{x_1, \dots, x_n\}$ satisfy the property that if x_i influences x_j , then x_j does not influence x_i . This means that the network nodes can be arranged in a sequence $x_1 \rightarrow x_2 \rightarrow \dots \rightarrow x_n$ (potentially by relabeling) such that no element influences another to its left. In such a dynamical system where $\dot{x}_i = f_i(\{x_1, \dots, x_i\}, t)$, the Jacobian ($J_{ij} = \partial f_i / \partial x_j$) is lower triangular. We make the following assumptions, which are appropriate for biochemical systems: i) The diagonal elements of J are negative, specifically, the degradation rates have strictly positive lower bounds (i.e., $\partial f_i(\{x_1, \dots, x_i\}, t) / \partial x_i \leq -c_i^2 < 0$), because every species is degraded in a concentration-dependent manner and the degradation rates do not vanish, at least, when the system is stimulated periodically. Linear degradation terms $\sim -k_i x_i$ and Michaelis-Menten terms $\sim -k_i x_i / (1 + x_i / x_{i0})$ (assuming x_i is bounded from above) fulfill this requirement, as well as Michaelis-Menten terms with Hill coefficients $\sim -k_i x_i^n / (1 + x_i^n / x_{i0}^n)$, where n reflects cooperativity $n > 1$ and x_i is bounded from below, e.g., due to the periodic stimulation. ii) The off-diagonal elements of J are bounded, i.e., all $|J_{ij}| < p_{\max}$.

Theorem 1: A feedforward system satisfying these two conditions has a unique periodic solution with period T (same as stimulus), to which every other solution converges. (For additional technical conditions, see Theorem 2 in ref.⁴⁵.)

Proof: By choosing a diagonal matrix P with $P_{ii} = 1/p^i$, we can make the off-diagonal elements of PJP^{-1} arbitrarily close to zero, the larger $p \gg p_{\max}$ is. Then, the matrix measures μ_1 , μ_2 , or μ_∞ , associated with the L^1 , L^2 , or L^∞ -norms, respectively, of PJP^{-1} are all approximately equal to the largest (i.e. least negative) diagonal element. Thus, the system is infinitesimally contracting with a positive contraction rate, and by theorem 2 in ref.⁴⁵, all $x_i(t)$ are T -periodic. \square

2.2 Positive feedback loops

The previous theorem pertains to feedforward systems without any closed loops, i.e., no influence of downstream nodes on upstream nodes. This leaves open the possibility of period skipping in systems which contain positive feedback loops (PFLs) as well as IFFLs. Such PFLs would have to be entirely

upstream or downstream of any IFFLs in the signal transduction cascade because a connection from the adapting node or its downstream nodes back upstream of the adapting node would create a NFL. So, we consider PFLs feeding into an IFFL feeding into another system of PFLs, and we wish to show that the composite system cannot show period skipping.

A few definitions and previous results are needed. By a system of PFLs ($\dot{\vec{x}}(t) = \vec{f}(\vec{x}(t), \vec{u}(t))$), we mean specifically that the two inequalities

$$\frac{\partial f_i}{\partial x_j}(\vec{x}, \vec{u}) \geq 0 \quad \forall i \neq j \quad \text{and} \quad \frac{\partial f_i}{\partial u_j}(\vec{x}, \vec{u}) \geq 0 \quad \forall i, j$$

hold for all \vec{x} and stimuli \vec{u} . The former inequality implies that the elements in the system only influence each other positively, i.e., lead to each other's increase, and the latter condition that the stimulus $\vec{u}(t)$ influences the elements of the system only positively as well. Systems satisfying the former condition are 'cooperative'. Thus, by PFLs we not only mean that the dynamic nodes increase each other but also that the input, e.g., the applied external stimulus, only increases the nodes that it influences directly.

Such systems are 'monotone'⁴⁶:

$$\vec{x}^{(1)}(t_0) \geq \vec{x}^{(2)}(t_0), \vec{u}^{(1)}(t) \geq \vec{u}^{(2)}(t) \quad \forall t \geq t_0 \quad \text{implies} \quad \vec{x}^{(1)}(t) \geq \vec{x}^{(2)}(t) \quad \forall t \geq t_0 \quad . \quad (1)$$

(For simplicity, we abbreviate the component-wise inequality $x_i \geq y_i$ for all vector components i by $\vec{x} \geq \vec{y}$.) Monotonicity is a more general condition on dynamics; here, we study the special cases of cooperative systems (with inputs).

An important result for periodically forced monotone systems $\dot{\vec{x}} = \vec{f}(\vec{x}(t), \vec{u}(t))$ is given as Theorem 5.26 in [Hirsch2005], which credits the unpublished 1997 Ph.D. thesis by I. Tereščák. This result applies to systems that are irreducible, meaning that all its Jacobian matrices are irreducible (i.e., every variable can indirectly affect every other variable, possibly through an arbitrary number of intermediates; see also [Hirsch 2003]). The result states that $\vec{x}(t)$ converges to a solution with period kT , where $k \geq 1$ is an integer, for almost all initial conditions if the stimulus $\vec{u}(t)$ is periodic with period T ($\vec{u}(t) = \vec{u}(t+T)$). It is important to note that, generally, there may be stable periodic solutions with period kT and $k > 1$, as shown in [Takac 1992]. Thus, we present additional conditions, appropriate for biological systems, which insure that $k = 1$. Since the set of initial conditions which lead to non- kT -periodic solutions has measure

zero, we consider those cases negligible for our purposes.

2.2.1 2D positive feedback loops

First, we show that a PFL, which only contains two dynamical elements and which is stimulated with period T , if it has a solution with period kT , where k is an integer, then k equals 1; thus, period skipping with $k = 2, 3, \dots$ is not possible. A related result exists in the literature: All 2D periodic irreducible cooperative systems approach a T -periodic solution [Hale 1983], which excludes chaotic solutions and noninteger k as well. Regardless, we present the following lemma and corollary because the proofs are self-contained and build towards the results in the subsequent section, and also because we do not need to assume irreducibility:

Lemma 1: Consider a 2D dynamical system, driven by an input of period T , ($\dot{\vec{x}}(t) = \vec{f}(\vec{x}(t), \vec{u}(t))$ where $\vec{x}(t) \in \mathbb{R}_+^2$ and $\vec{u}(t) = \vec{u}(t + T)$), and suppose that $\vec{x}(t_0)$ is a periodic point with some period kT , where k is a positive integer. Then there is some time t_1 so that $\vec{x}(t_1) \leq \vec{x}(t_1 + T)$ or some time t_2 so that $\vec{x}(t_2) \geq \vec{x}(t_2 + T)$.

Proof: Suppose without loss of generality that $t_0 = 0$ and that (otherwise we are done, with $t_1 = 0$) $x_1(0) > x_1(T)$ and $x_2(0) < x_2(T)$ (if the opposite inequalities hold, the argument is analogous). There is some integer $s > 1$ so that $x_1((s-1)T) \leq x_1(sT)$ since, otherwise, $x_1((s-1)T) > x_1(sT)$ for all s , and therefore $x_1(0) = x_1(kT) < x_1((k-1)T) < \dots < x_1(0)$, which is a contradiction.

Now pick any such s and let $S = (s-1)T$. Then, the continuous function $p(t) := x_1(t) - x_1(t+T)$ has $p(0) > 0$ and $p(S) \leq 0$, so there is some minimal t_1 so that $p(t_1) = 0$.

Similarly, consider $q(t) := x_2(t) - x_2(t+T)$, which has $q(0) < 0$, and conclude that there is some minimal t_2 so that $q(t_2) = 0$. Suppose that $\min\{t_1, t_2\} = t_1$. Then $x_1(t_1) = x_1(t_1 + T)$ and $x_2(t_1) \leq x_2(t_1 + T)$. If instead $\min\{t_1, t_2\} = t_2$, then the other inequality holds. \square

Before proving the following corollary, we introduce the notation $F(\vec{x}(s)) = \vec{x}(s+T)$ for the solution to the differential equation $\dot{\vec{x}}(t) = \vec{f}(\vec{x}(t), \vec{u}(t))$ at time $s+T$ starting with initial condition $\vec{x}(s)$ at time s . Furthermore, we denote by $F^k(\vec{x}(s)) = \underbrace{F \circ \dots \circ F}_{k \text{ times}}(\vec{x}(s))$ the k -fold mapping of the initial condition $\vec{x}(s)$. Note that $F^k(\vec{x}(s)) = \vec{x}(s+kT)$, which we prove by induction: For $k = 1$, it follows from the definition. Next, assuming that $F^n(\vec{x}(s)) = \vec{x}(s+nT)$ holds, we define $\vec{z}(t) = \vec{x}(t+nT)$ and note that $\dot{\vec{z}}(t) = \dot{\vec{x}}(t+nT) = \vec{f}(\vec{x}(t+nT), \vec{u}(t+nT)) = \vec{f}(\vec{z}(t), \vec{u}(t))$, where the last equality follows from the

definition of \vec{z} and the periodicity of \vec{u} . So, like $\vec{x}(s)$ before, we can map $\vec{z}(s)$ forward in time by one period $\vec{z}(s+T) = F(\vec{z}(s)) = F(F^n(\vec{x}(s))) = F^{n+1}(\vec{x}(s))$, and, also, $\vec{z}(s+T) = \vec{x}(s+nT+T) = \vec{x}(s+(n+1)T)$. Thus, we have $F^{n+1}(\vec{x}(s)) = \vec{x}(s+(n+1)T)$. \square

Using this notation and the monotonicity property, we prove the following:

Corollary: Suppose the system is monotone, in addition to the conditions in Lemma 1, and $\vec{x}(t)$ is periodic with period kT ($\vec{x}(t) = \vec{x}(t+kT)$), then $\vec{x}(t+T) = \vec{x}(t)$ for all t , i.e., the orbit of \vec{x} has period T .

Proof: The mapping F is monotone by assumption (Eq. (1)). We pick the time t_1 as in Lemma 1 (the proof would be analogous with t_2), so $\vec{x}(t_1) \leq F(\vec{x}(t_1))$. By monotonicity, the inequality is preserved under repeated mappings, $F^n(\vec{x}(t_1)) \leq F^{n+1}(\vec{x}(t_1))$. So, iterating, $\vec{x}(t_1) \leq \vec{x}(t_1+T) \leq \vec{x}(t_1+2T) \dots \leq \vec{x}(t_1+kT) = \vec{x}(t_1)$, where the last equality comes from the assumption that $\vec{x}(t)$ has period kT . Since $\vec{x}(t_1) = \vec{x}(t_1+T)$, we have $\vec{x}(t) = \vec{x}(t+T)$ for all times t . \square

2.2.2 Positive feedback loops stimulated from rest

Next, we consider systems of PFLs $\dot{\vec{x}}(t) = \vec{f}(\vec{x}(t), \vec{u}(t))$ with $\vec{x}(t)$ consisting of any finite number of components, i.e., not restricted to two as in the previous section. We show that period skipping trajectories are inaccessible to the system if it is initially at rest before periodic stimulation, even if the PFL system could exhibit period skipping in principle.

First, we note that a non-negative stimulus always raises the concentrations of the components of a PFL system relative to the steady state where the stimulus is off: From the monotonicity property in Eq. (1), we have that $\vec{x}^{(1)}(t) \leq \vec{x}^{(2)}(t)$ for all $t \geq 0$ if the systems starts from the same initial state $\vec{x}(0)$ and if the inputs satisfy $\vec{u}^{(1)}(t) \leq \vec{u}^{(2)}(t)$ for all $t \geq 0$. So, if we compare the steady state (i.e. with input $\vec{u}^{(1)}(t) = 0$) to the system after the onset of stimulation, i.e., $\vec{u}^{(2)}(t)$ is non-negative for all $t \geq 0$, and $\vec{x}(0) = \vec{x}_{ss}$ is the steady state, it follows that $\vec{x}_{ss} = \vec{x}^{(1)}(t) \leq \vec{x}^{(2)}(t)$ for all $t \geq 0$.

In the following, we imagine that \vec{x} is the state of the system after sufficiently many stimulus pulses, starting from \vec{x}_{ss} initially, such that the solution has converged to a kT -periodic solution (and we show that $k = 1$):

Theorem 2: Let F (introduced in the previous section) be a monotone mapping. Suppose that these properties hold for two fixed states \vec{x} and \vec{x}_{ss} :

$$(1) \quad \vec{x}_{ss} \leq F(\vec{x})$$

(2) $F^k(\vec{x}) = \vec{x}$ for some integer $k \geq 1$

(3) $F^l(\vec{x}_{ss}) - F^l(\vec{x}) \rightarrow 0$ as $l \rightarrow \infty$

Then $F(\vec{x}) = \vec{x}$.

Proof: Pick an integer $n \geq 0$. Then, for any integer $r \geq 1$:

$$F^n(\vec{x}) = F^{rk+n}(\vec{x}) = F^{rk+n}(\vec{x}) - F^{rk+n}(\vec{x}_{ss}) + F^{rk+n}(\vec{x}_{ss}) \leq q_r + F^{rk+n+1}(\vec{x}) = q_r + F^{n+1}(\vec{x})$$

where $q_r = F^{rk+n}(\vec{x}) - F^{rk+n}(\vec{x}_{ss})$ and where we used (2) to obtain $F^n(\vec{x}) = F^{rk+n}(\vec{x})$, then (1) to get $F^{rk+n}(\vec{x}_{ss}) \leq F^{rk+n}(F(\vec{x})) = F^{rk+n+1}(\vec{x})$ and finally again (2) to get $F^{rk+n+1}(\vec{x}) = F^{n+1}(\vec{x})$. Using (3), $q_r \rightarrow 0$ as $r \rightarrow \infty$, so we conclude that $F^n(\vec{x}) \leq F^{n+1}(\vec{x})$ for all $n \geq 0$.

Thus,

$$\vec{x} \leq F(\vec{x}) \leq F^2(\vec{x}) \leq \dots \leq F^k(\vec{x}) = \vec{x} \quad ,$$

and therefore $F(\vec{x}) = \vec{x}$. \square

Theorem 2 ensures that, if a system is monotone and the input is periodic with period T , then the solution when starting from a steady-state cannot approach a periodic orbit of (minimal) period kT , where $k > 1$ is an integer.

2.2.3 Composite PFL \rightarrow IFFL \rightarrow PFL systems

Stitching together our mathematical results for purely feedforward systems and PFLs, we see that period skipping is impossible in a composite $S \rightarrow$ PFL \rightarrow IFFL \rightarrow PFL system, where $S(t)$ is the applied periodic on-off stimulus ($= \vec{u}(t)$ in the above proofs for the first PFL in the signaling cascade). This leaves period skipping generically to NFLs. There are, however, two subtleties:

In the first step of the cascade ($S \rightarrow$ PFL) the above proofs apply exactly but in the subsequent steps (PFL \rightarrow IFFL and IFFL \rightarrow PFL), the input is no longer exactly periodic but converges to a periodic function of time. While this may be a concern in general, here it is not: i) For a contractive system such as the purely feedforward system described above, if the stimulus approaches the periodic stimulus $\vec{u}(t)$, the solution approaches the periodic solution $\vec{x}(t)$ for stimulus $\vec{u}(t)$. This follows from the main results in [Desoer 1972] and more generally the theory developed in [Aminzare 2014]. Thus, for the PFL \rightarrow IFFL step, our previous result of no-skipping in purely feedforward systems continues to hold. ii) Similarly, for

monotone systems such as the PFLs, the solution approaches the solution $\vec{x}(t)$ for the periodic stimulus $\vec{u}(t)$ if the stimulus approaches $\vec{u}(t)$. This property is the analogue, for stable periodic orbits instead of stable steady states, of the “convergent input convergent state property” for monotone systems which was treated in ref. ⁴⁶. We omit the proof, which is similar. Thus, for the IFFL \rightarrow PFL step, our result of no-skipping in 2D or no-access to skipping in general PFL systems continues to hold as well.

Another issue is that in our definition of PFLs, we assumed that the stimulus only influences the nodes of the PFL positively. While this is a straightforward assumption for the first step in the cascade ($S \rightarrow$ PFL), it also has to hold for the way the IFFL feeds the final PFL (IFFL \rightarrow PFL). If it does not hold, the system may contain additional adapting circuits and a further break-down into subcircuits is necessary for the analysis.

3 Published models

To decide whether any individual adaptation mechanism is an IFFL or NFL, one has to examine whether the adaptation mechanism is direct/independent of the response R (IFFL) or indirect/dependent on the response R (NFL).

3.1 State-dependent inactivation model

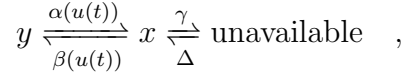
The dynamical system in ref. ⁹,

$$\begin{aligned}\dot{x} &= \alpha(u(t))(A - x) - \beta(u(t))x - \gamma x + \Delta \\ \dot{A} &= -\gamma x + \Delta,\end{aligned}$$

where x is the active species and A the sum of the active species x and the inactive species $y (= A - x)$, can be rewritten in terms of x and y ,

$$\begin{aligned}\dot{x} &= \alpha(u(t))y - \beta(u(t))x - \gamma x + \Delta \\ \dot{y} &= \beta(u(t))x - \alpha(u(t))y.\end{aligned}$$

This transformation just re-expresses the central reactions in the Friedlander-Brenner scheme,



in terms of x and y instead of x and the sum $A = x + y$.

For perfect adaptation, Δ is chosen to be constant, as in Fig. 2 E-F in ref.⁹. There is clearly no NFL in the system, since x and y influence each other positively (assuming that $\alpha(u(t)), \beta(u(t)) > 0$, as in ref.⁹). The circuit adapts because $\alpha(u(t))$ turns on x directly (in a y -dependent manner), but reduces y directly (**independently of x**) as well, leading to the subsequent decay of x . This is clearly an IFFL, and it is the same basic mechanism as in the IFFL circuit B in Fig. 1 or IFFL 4 in Fig. S2 with $x \rightarrow R$ and $y \rightarrow X$ roughly analogous. This may be a difficult case for recognizing the IFFL topology because the depletion of y and build-up of x are linked molecularly in the same process, but that does not change the basic mechanism of the IFFL circuit, in which $\alpha(u(t))$ builds up x and depletes y directly (**independently of x**), the latter being responsible for adaptation. Of course, our IFFL models do not have the additional features of the Friedlander-Brenner model such as a positive feedback loop.

We used the model and parameters in Fig. 2 E-F of ref.⁹ to verify that this model neither shows periodic skipping nor refractory period stabilization, as expected for an IFFL. To observe the refractory period, we chose as output nonlinearities $O(d, T) = \langle x^2 \rangle$ or $O(d, T) = \langle x^3 \rangle$.

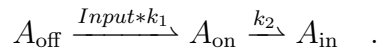
In ref.¹⁰, the state-dependent inactivation model was presented in a simpler form:

$$\begin{aligned} \dot{A}_{\text{on}} &= k_1 \text{Input} (1 - A_{\text{on}} - A_{\text{in}}) - k_2 A_{\text{on}} \\ \dot{A}_{\text{in}} &= k_2 A_{\text{on}}, \end{aligned}$$

where the input converts protein $A_{\text{off}} = (1 - A_{\text{on}} - A_{\text{in}})$ into the ‘on’ form of the protein A_{on} , which is slowly converted into the inactive form A_{in} . This system adapts perfectly to a step input. To analyze the system further, we rewrite the equations in terms of A_{on} and A_{off} instead of A_{on} and A_{in} :

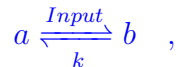
$$\begin{aligned} \dot{A}_{\text{on}} &= k_1 \text{Input} A_{\text{off}} - k_2 A_{\text{on}} \\ \dot{A}_{\text{off}} &= -k_1 \text{Input} A_{\text{off}}. \end{aligned}$$

Both sets of equations of course describe the same reactions, only the transformed (latter) set describes the dynamics of A_{on} and A_{off} , which are central to the adaptation mechanism:



As in the above case of the Friedlander-Brenner model, this system can be identified as an IFFL because the input increases A_{on} directly and at the same time decreases A_{off} directly (independently of A_{on}), which thus decreases A_{on} again, leading to adaptation. This too may be a difficult case for recognizing the IFFL topology because the depletion of A_{off} and build-up of A_{on} are linked molecularly in the same process, but that does not change the basic mechanism of the IFFL circuit, in which the *Input* builds up A_{on} and depletes A_{off} directly (independently of A_{on}), the latter being responsible for adaptation. Using the parameters in ref.¹⁰ ($k_1 = 1$ and $k_2 = 1$), a constant influx into A_{off} to allow recovery ($\dot{A}_{\text{off}} = 1 - k_1 \text{Input} A_{\text{off}}$), an input that jumps from 0.01 (off) to 1 (on), and a nonlinearity $O(d, T) = \langle A_{\text{on}}^3 \rangle$ to observe a refractory period, we could not detect refractory period stabilization or period skipping in this system either, as in the above Friedlander-Brenner model and as expected for an IFFL.

We also note here for comparison that a simple phosphorylation/dephosphorylation system,



technically an IFFL, does not produce adaptation. Modifications such as the introduction of a third species as in the Friedlander-Brenner model are necessary to make this an adapting system.

3.2 Fold-change detection models

We used the models in Fig. 1 B, C in ref.²⁶, rewritten in terms of dimensionless parameters as in Eqns. (5) and (6) of ref.²⁶ with model parameters $T = 1$ and $T = 10$ for the IFFL model and the NFL model, respectively, as in Figs. 3 and 4 of ref.²⁶. We found period skipping for the NFL model with pulse width $d = 0.2$ and pulse period 5, but neither period skipping nor refractory period stabilization in the IFFL model. We also switched the parameters (model parameter $T = 1$ for the NFL model or model parameter $T = 10$ for the IFFL model) and found the same results. Since an off stimulus $S = 0$ is

difficult to implement computationally with these models, we chose $S = 0.001$ as our off stimulus (and $S = 1$ as usual for the on stimuli). To observe the refractory period, we chose as an output nonlinearity $O(d, T) = \langle y^2 \rangle$.

Supplementary Tables

circuit type	total # tested	# adapting	# skipping + # refrac. period stabilization
NFL	1152	391	279 (71%)
IFFL	1152	382	0 (0%)

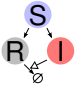
Table S1:

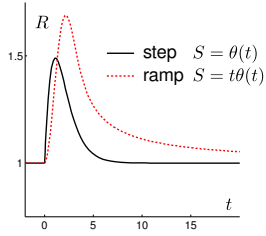
Refractory period stabilization and period skipping in NFLs do not require step thresholds. We took the models in Fig. 1 E, F (same as I, J) and replaced $\theta(I_0 - I)$, which shuts off the stimulus S when the inhibitor $I(t)$ exceeds the threshold I_0 in an all-or-nothing fashion, by $1/(1+(I/I_0)^n)$ where $n \in \{1, 2, 3, 4\}$ and $I_0 \in \{0.01, 0.1, 1, 10\}$ as well as the output function $O = R$ by $\dot{O} = R^m/(1+(R/R_0)^m) - \lambda_O O$ where $m \in \{1, 2\}$ and $R_0 \in \{0.1, 1, 10, \infty\}$ or $m = 3$ and $R_0 = \infty$. λ_O is irrelevant for T_{\max} . We varied $\lambda \in \{0.01, 0.02, 0.03, 0.1, 0.2, 0.3, 1.0, 10\}$. Overall, we varied parameters over 3 orders of magnitude, and read out 9 different variations of the output function. For details, see Methods.

Supplementary Figures

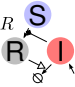
Adaptation to linear ramps

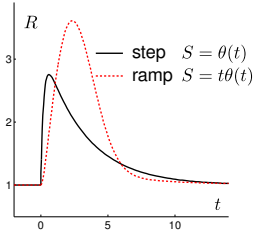
A IFFL

$$\begin{aligned} \dot{R} &= S - IR \\ \dot{I} &= S - I \end{aligned}$$




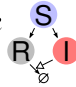
B NFL

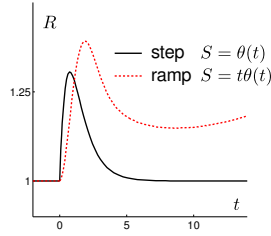
$$\begin{aligned} \dot{R} &= (S + .5)X - 5R \\ \dot{X} &= 1 - R \end{aligned}$$




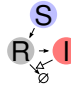
Lack of adaptation to linear ramps

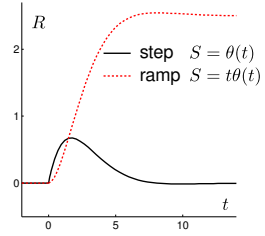
C IFFL

$$\begin{aligned} \dot{R} &= S - \frac{2I}{1+I/10}R \\ \dot{I} &= S - \frac{2I}{1+I/10} \end{aligned}$$




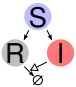
D NFL

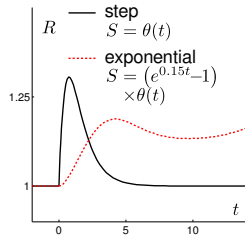
$$\begin{aligned} \dot{R} &= S - AI - R \\ \dot{I} &= R \end{aligned}$$




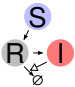
Lack of adaptation to exponentials

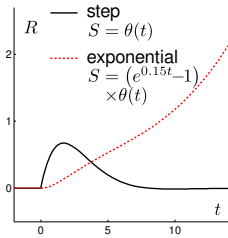
E IFFL

$$\begin{aligned} \dot{R} &= S - \frac{2I}{1+I/10}R \\ \dot{I} &= S - \frac{2I}{1+I/10} \end{aligned}$$




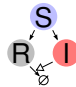
F NFL

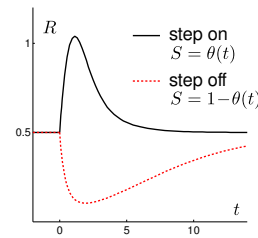
$$\begin{aligned} \dot{R} &= S - AI - R \\ \dot{I} &= R \end{aligned}$$




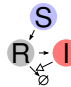
Overshoot when input switched off

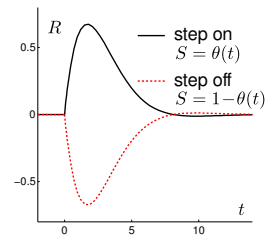
G IFFL

$$\begin{aligned} \dot{R} &= S - IR + .1 \\ \dot{I} &= S - .5I + .1 \end{aligned}$$




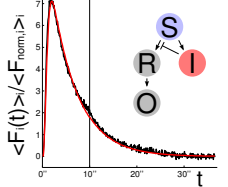
H NFL

$$\begin{aligned} \dot{R} &= S - AI - R \\ \dot{I} &= R \end{aligned}$$




Fit to data

I IFFL

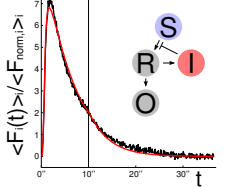


$$\begin{aligned} \dot{R} &= a_1 \left(\frac{S}{1 + \left(\frac{I}{I_0}\right)^{n_1}} - l_1 R \right) \\ \dot{I} &= a_2 (S - l_2 I) \\ \dot{O} &= a_3 (R^{n_3} - l_3 O) \end{aligned}$$

$a_1 = 0.934...$ $l_1 = 0.715...$
 $a_2 = 0.162...$ $l_2 = 1.90... \cdot 10^{-4}$
 $a_3 = 0.00935...$ $l_3 = 1.95...$
 $n_1, N_0 = 3.00...$ $n_3 = 3.01...$

RMSD = 0.167

J NFL



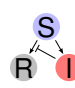
$$\begin{aligned} \dot{R} &= a_1 \left(\frac{S}{1 + \left(\frac{I}{I_0}\right)^{n_1}} - l_1 R \right) \\ \dot{I} &= a_2 (R^{n_2} - l_2 I) \\ \dot{O} &= a_3 (R^{n_3} - l_3 O) \end{aligned}$$

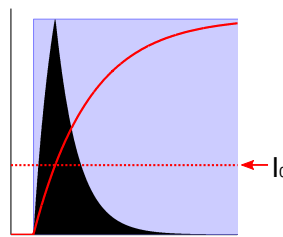
$a_1 = 0.842...$ $l_1 = 0.675...$
 $a_2 = 0.143...$ $l_2 = 1.00... \cdot 10^{-4}$
 $a_3 = 0.0117...$ $l_3 = 1.97...$
 $N_0 = 3.00...$ $n_2 = 2.96...$
 $n_1 = 3.04...$ $n_3 = 3.06...$

RMSD = 0.152

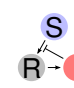
Continuous stimulus

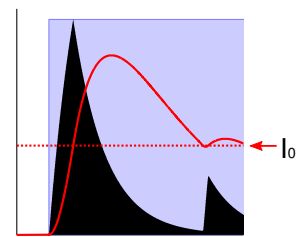
K IFFL

$$\begin{aligned} \dot{R} &= S\theta(I_0 - I) - R \\ \dot{I} &= S - \lambda I \end{aligned}$$


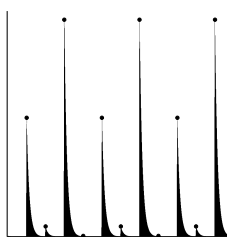


L NFL

$$\begin{aligned} \dot{R} &= S\theta(I_0 - I) - R \\ \dot{I} &= R - \lambda I \end{aligned}$$




M skipping



N skipping

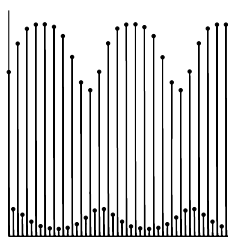


Figure S1: (Caption on next page.)

Examples showing that IFFLs and NFLs can show qualitatively similar responses to linearly ramping, exponentially ramping, or on-off stimuli (A-H), fits to the same experimental data (I, J), examples showing the behavior of the circuits in Fig. 1 E, F (same as Fig. 1 I, J) under continuous stimulation (K, L), and examples of period skipping for NFLs (M, N). A-H: Examples showing that various response characteristics from the literature can appear in both IFFLs and NFLs. Adapted from refs.^{8,19-23} $\theta(t)$ is a step function, which is zero for $t < 0$ and equal to one for $t > 0$. The linear ramp $t\theta(t)$ is equal to t for $t > 0$ and equal to zero for $t < 0$. The exponential ramp $(e^{xt} - 1) \times \theta(t)$ is equal to $(e^{xt} - 1)$ for $t > 0$ and equal to zero for $t < 0$. A, B: Adaptation to step inputs and linear ramps; C, D: adaptation to step inputs but failure to adapt to linear ramps; E, F: adaptation to step inputs but failure to adapt to exponential ramps; G, H: overshoot below steady-state when the input is turned off (red dashed line, switch $S = 1$ to $S = 0$ at $t = 0$). I, J: Black: The 15'th response pulses at odor pulse duration $d = 10''$ and period $T = 42''$ were taken from our *C. elegans* recordings, averaged over all worms, and then normalized to the mean of the 9'th and 10'th response pulses. Red: We guessed parameters for each model and then fine-tuned them to the data by a steepest-descent algorithm minimizing the root mean square deviation (RMSD). K, L: With long stimulus (S) pulses (blue), the response R is effectively shut off from the stimulus S when I exceeds I_0 in the model circuits in Fig. 1 E, F (same as Fig. 1 I, J). In the NFL circuit, I can drop below I_0 again while the stimulus is on, allowing the stimulus S to cause another spike in R , and repeat. However, softening the step inhibition function (here: $\theta(I_0 - I)$) easily abolishes sustained oscillations (not shown). For the model calculations in Fig. 1 J, we plot $T_{\max}(d)$ for pulse durations d before there is a second response spike elicited by the same stimulus pulse. M, N: Examples of period skipping with $4T$ -periodic (M, one NFL) or more complicated (N, interlocking NFLs) responses to T -periodic stimuli. Peaks are marked by black circles. Periodic stimuli are not shown.

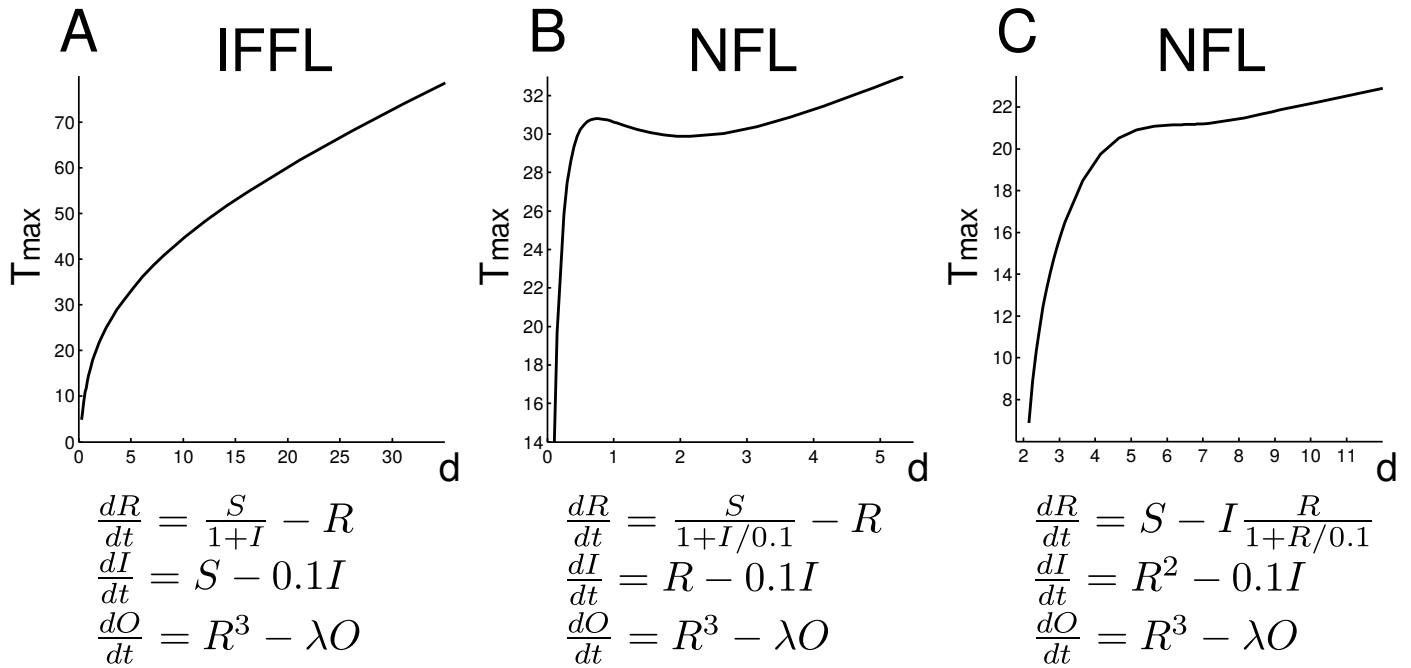


Figure S3:

Examples of $T_{\max}(d)$ plots from the computational search summarized in Table 1. A-C: λ is arbitrary. A: An IFFL model with simple (non-cooperative) Michaelis-Menten inhibition. B: An NFL model with simple (non-cooperative) Michaelis-Menten inhibition showing that $T_{\max}(d)$ can even have a negative slope. C: An NFL model in which the inhibitor I degrades the response R .

$$\dot{R} = S\theta(I_0 - I) - R, \quad \dot{I} = R - \lambda I, \quad O = R$$

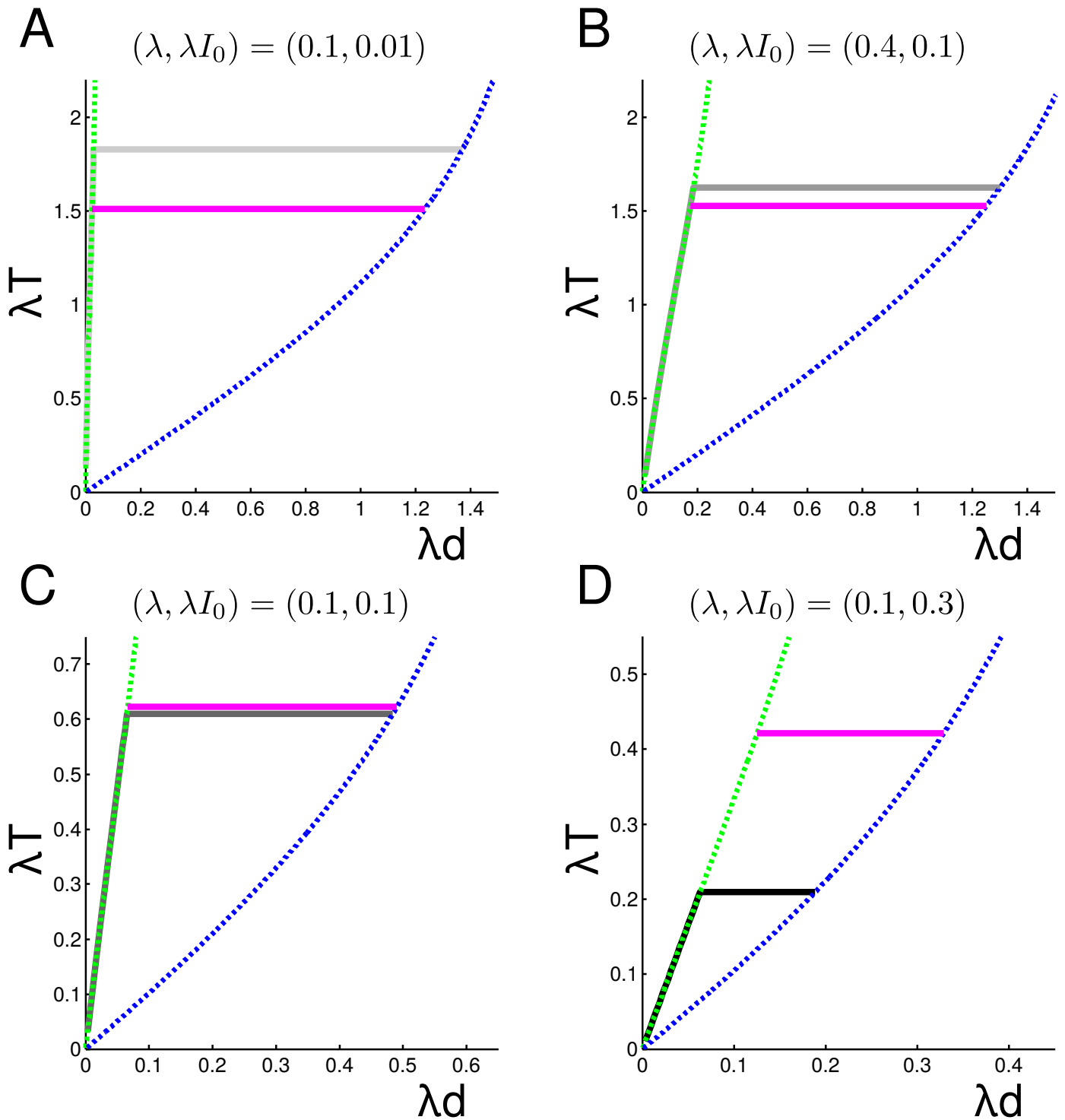


Figure S4:

Detailed analysis of NFL circuits in Fig. 1 J showing that $T_{\max}(d)$ (grey lines) and pulse periods

and widths leading to period skipping (magenta-green-blue triangles below magenta lines) are close for a variety of model parameters. Thus, a search for T_{\max} may be expected to lead to observing period skipping as well, if it occurs.

Grey lines: $T_{\max}(d)$ plotted with the same shades of grey as in Fig. 1 J.

Magenta lines: In the triangles between the green, blue, and magenta lines (below the magenta lines), periodic solutions with the same period T as the stimulus period are unstable and period skipping is observed.

Blue dashed lines: The regions of interest for our analysis are to the left of the blue dashed lines in each panel; to the right of the blue dashed lines, each stimulus pulse is so long that the circuits respond at least twice to each stimulus pulse (R goes up at least twice), because each stimulus pulse extends beyond the time when the circuit recovers from adaptation, i.e., when I drops below I_0 again, and can be activated again. This may be a feature of these models that is not observed in many biological NFLs and thus we refrain from analyzing the models in this regime.

Green dashed lines: To the left of the green dashed lines, the pulse durations d are too short (alternatively, the pulse periods T too long) for enough inhibitor I to accumulate during each periodic stimulus pulse to block the stimulus pulses at all and thus for the responses to show any adaptation; $\theta(I_0 - I)$ is always equal to 1. To the right of the green dashed lines, the pulse durations d are long enough (alternatively, the pulse periods T short enough) for enough inhibitor to accumulate during each stimulus pulse to block the stimulus pulses at some point after the onset of each stimulus pulse. For any fixed pulse period T , making the pulse durations d longer than specified at the green boundary has the same effect as stimulus pulses with pulse durations at the green boundary because the inhibitor cuts the stimulus off ($\theta(I_0 - I) = 0$) for pulse durations to the right of the boundary line.

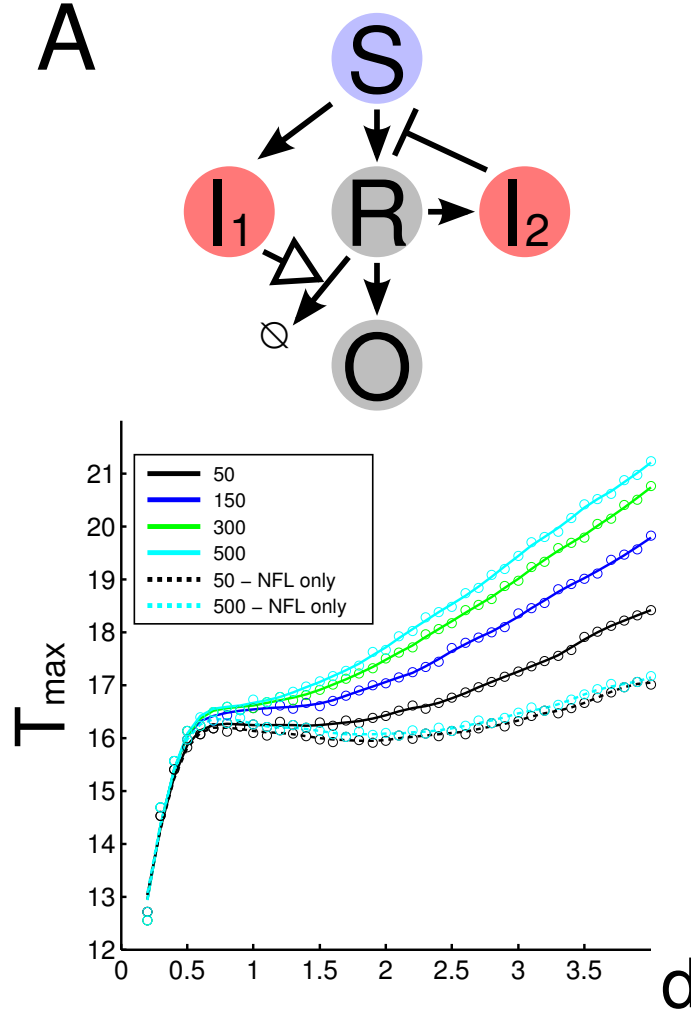


Figure S5:

A: $T_{\max}(d)$ for a pathway combining an IFFL circuit (through I_1) with slower kinetics and an NFL circuit (through I_2) with faster kinetics, acting in parallel. After the onset of on-off pulsing, the NFL circuit influences the output quickly whereas the IFFL circuit affects the output more slowly. So, we measured the running average of the output ($= O(d, T)$) at different time points 50, 150, . . . after the onset of the periodic on-off stimulus. For the NFL-only circuit (I_2 set to 0, dashed lines), which is presented for comparison, $T_{\max}(d)$ is strongly stabilized and in fact decreases at intermediate d . In the full circuit, as $O(d, T)$ is defined at later time points, T_{\max} stabilization slowly disappears (black \rightarrow blue \rightarrow green \rightarrow cyan). ($\dot{I}_1 = S - \lambda_1 I_1$, $\dot{I}_2 = R - \lambda_2 I_2$, $\dot{R} = S/(1 + (I_2/I_0)^n) - (1 + \kappa I_1)R$, $O(t) = R^3(t)$, $\lambda_1 = 1/200$, $\lambda_2 = 2/10$, $\kappa = 1/100$, $n = 1$, $I_0 = 1/10$)

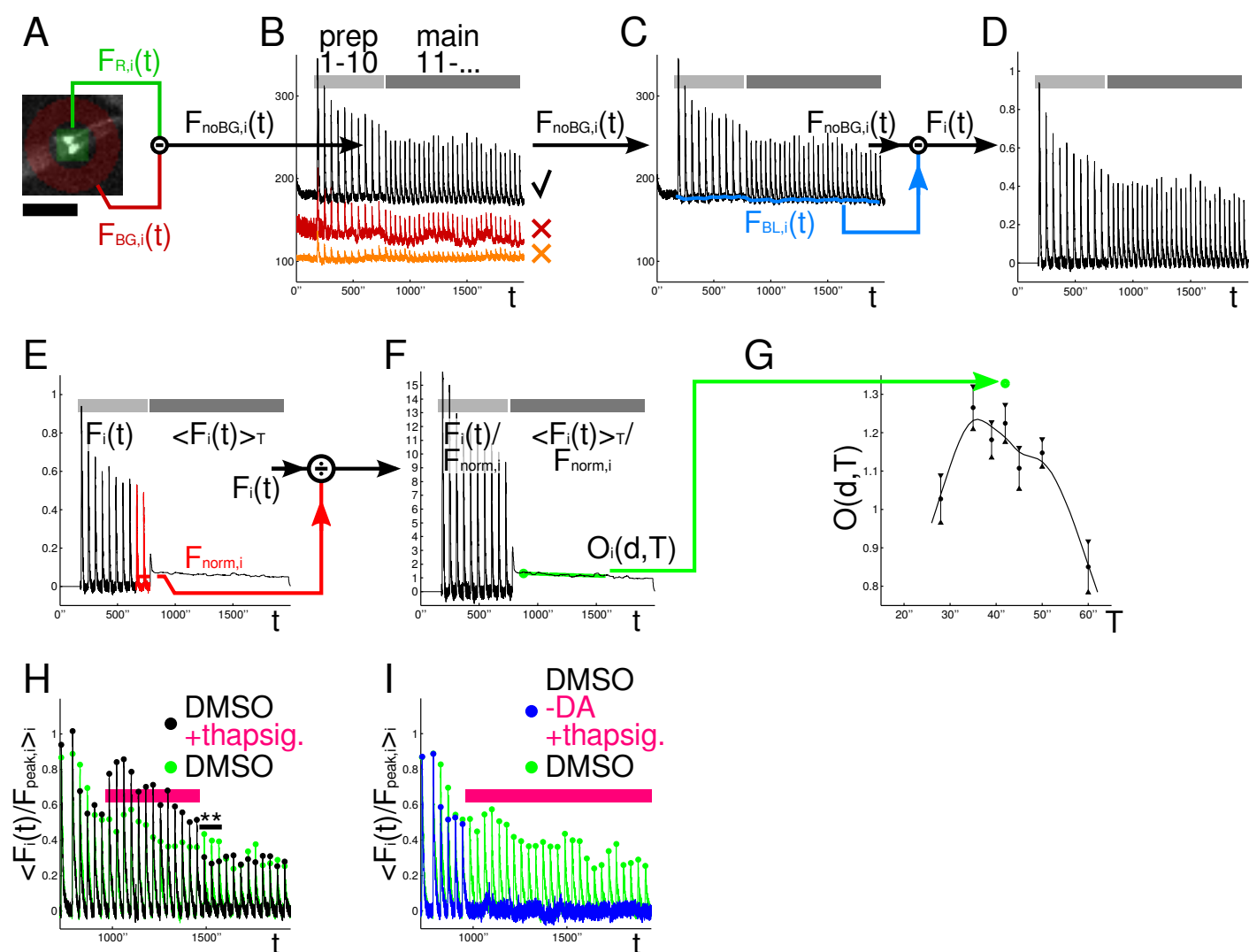


Figure S6:

Processing of *C. elegans* experimental data and additional pharmacological experiments. For details, see Methods. In all experiments, the main odor pulses (here: $d = 20''$, $T = 42''$) were preceded by 10 preparatory odor pulses of duration $10''$ and period $60''$. A: One imaged frame (cropped, of about 20000 total frames per experiment, recorded at 10 Hz) showing GCaMP fluorescence from the AWA neuron pair of a single worm. $F_{R,i}(t)$ is the average intensity over the area indicated by a green square, centered on the AWA neurons, and $F_{BG,i}(t)$ is the median intensity over the region indicated by a red ring. Scale bar: $100\mu m$. B: $F_{noBG,i}(t) = F_{R,i}(t) - F_{BG,i}(t)$ plotted for different worms from the same experiment. The red trace is filtered out because the baseline moves too much (6.5%) before and after the preparatory odor pulse 10. The orange trace is discarded because the noise-to-signal ratio (0.11-0.15) is too high. See Methods for more details. C: A piecewise linear function $F_{BL,i}(t)$ (blue) representing

the time-dependent baseline fluorescence is fit through $F_{\text{noBG},i}(t)$ before each response pulse. D: Plot of $F_i(t) = F_{\text{noBG},i}(t)/F_{\text{BL},i}(t) - 1$, which is corrected for the baseline fluorescence $F_{\text{BL},i}(t)$. E: $F_i(t)$ is plotted for the preparatory pulses and its running average over a time window of size T is plotted for the main pulses. The mean of $F_i(t)$ over the preparatory pulses 9 and 10 ($= F_{\text{norm},i}$, area indicated in red divided by $120''$) is shown as a horizontal red bar. F: $F_i(t)$ is normalized by $F_{\text{norm},i}$; then, the normalized running average is fit to a straight line between $100''$ - $800''$ after the beginning of the main odor pulses. G: The value of the linear fit at $100''$ after the beginning of the main odor pulses represents the output data point $O_i(d, T)$ for worm i at pulse duration d and period T . H, I: Fig. 3 I underlain for comparison. H: Same as Fig. 3 E except thapsigargin applied longer (for additional three odor pulse periods). Mean over 13 worms. I: Thapsigargin applied but odor stimulus pulses turned off. Thapsigargin presentation in the absence of odor only caused minor and brief increases in Ca^{2+} , potentially, by disrupting baseline Ca^{2+} maintenance. Mean over 14 worms.